DEVELOPING EXTINCTION CRITERIA FOR FIRES

J. W. Williamson, A. W. Marshall and A. Trouvé
Department of Fire Protection Engineering, University of Maryland
College Park, Maryland, 20742, USA

The scalar dissipation rate is widely used in combustion analysis to describe a characteristic transport time scale. This time scale is often used with Damköhler number arguments (describing the ratio of the mixing time to the chemical time) to determine if kinematic conditions within reacting flows will cause extinction. However, for extinction analysis in fires, transport time scales are assumed to be relatively long and flow effects are generally ignored. In the current study, transport time scales in fires and their associated scalar dissipation rates are explored analytically and computationally to determine if extinction events should be expected in fires and under what conditions they may occur. Particular attention is given to the compartment fire scenario where air vitiation effects will weaken flames and increase the probability of extinction. A model is presented which uses reactant composition and temperature in the vicinity of the flame to determine a modified (for vitiation) critical scalar dissipation rate for extinction. This model is based on vitiated laminar flame experiments and OPPDIF 1-D flame analysis conducted over a wide range of thermal, composition, and flow conditions. The experiments are performed with a novel counterflow slot burner producing flame sheets approaching extinction. The model is used to produce extinction maps for comparison with FDS to evaluate the validity of critical flame temperature models and the benefits of more general scalar dissipation rate based models for fire applications.

1. INTRODUCTION

The analysis of accidental fires poses a complex highly coupled multi-physics problem where the environmental conditions affecting fire behavior are strongly influenced by the fire behavior itself. Understanding the effect of these environmental conditions on the details of physical processes within the fire is required to develop properly coupled physical models for predicting fire dynamics. The dependence of the burning rate of the fire on the vitiated environment that it may produce is an important example of this coupling. In underventilated fires, smoke mixes with the air entrained by the fire resulting in oxidation of the fuel under vitiated conditions as illustrated in Figure 1. The elevated temperature and reduced oxygen content of the oxidizer stream can lead to fire behavior quite different from that expected when burning takes place with fresh air. In fact, vitiation may lead to incomplete combustion, local extinction, or even global extinction. It is also worth noting that fire
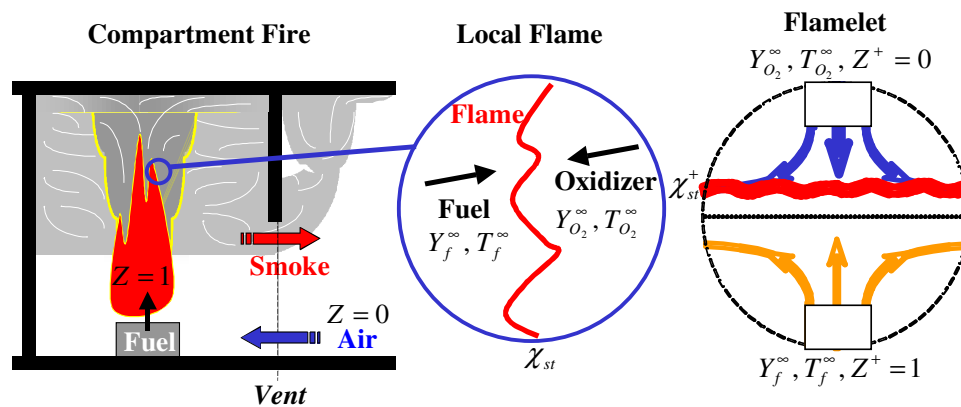

Figure 1: Compartment fire with air vitiation effects and the association between 1-D OPPDIF simulations to local flamelet behavior. Local reactants are affected by dilution ($Y_{O_2}^{\infty} \leq Y_{O_2,amb}$) and preheating ($T_{O_2}^{\infty} \geq T_{O_2,amb}$).

analysis is often performed to establish requirements for fire suppression or extinguishment. This fire abatement is commonly achieved by the displacement of oxygen either through reducing ventilation, inert gas discharge, or vaporization of water droplets. An extinction model is required to provide the necessary fidelity to accurately predict extinction in these reduced oxygen atmospheres.

Under-ventilated fires have received considerable attention by previous researchers. Earlier studies have focused on the behavior of severely under-ventilated fires [1, 2]. These studies have provided insight into the global fire phenomena that can occur when the oxygen supply to the fire is limited. Most recently, Utiskul classified the fire dynamics in scale model experiments into three burning modes, which include steady well-ventilated burning, steady under-ventilated burning, and unsteady under-ventilated burning [3]. Fundamental differences in the combustion process associated with these different burning modes must be quantified for accurate prediction of the associated fire dynamics. Some of these differences have already been explored through clever steady state experiments where turbulent diffusion flames were placed within an extended exhaust hood while ventilation was carefully adjusted until the experimental flame was partially or completely enveloped by its own exhaust [4, 5]. Measurements in these 'hood' experiments were performed to assess changes to exhaust gas composition and temperature under various ventilation conditions. The CO concentration in the exhaust gases and its relationship with the degree of ventilation were of particular interest in Beyler's experiments [4]. Beyler found that CO and UHC concentrations in the exhaust gases increased sharply for under-ventilated conditions with equivalence ratio, $\phi > 0.5$. On the other hand, Morehart et al. focused on fire behavior very close to extinction in completely enveloped fires [5]. They found that no soot was produced in flames very close to extinction in this basic configuration. This result is similar to observations made in Takeda [2] and Utiskul's [3] severely under-ventilated fires. Furthermore, Morehart et al. found that limiting oxygen concentrations and temperatures for their large scale fires compared favorably with laminar flame experiments. This result provided some evidence, albeit not yet with explanation, that extinction experiments using laminar flames may be suitable for studying large scale fire phenomenon.

Williams introduced the laminar flamelet concept providing a theoretical basis for the application of laminar flame experiments and analysis to characterize turbulent flame behavior [6]. This approach requires the flame thickness to be much smaller than turbulent eddies in the flow, which is easily satisfied in typical accidental fires. Motivated by this theory, numerous experiments and analysis have been conducted to evaluate extinction criteria in laminar flames [7-10]. The counterflow burner configuration has been employed extensively to generate laminar flames, providing the capability to control the flow condition, reactant composition, and even reactant temperature. Parallel analytical studies have been conducted in this configuration using asymptotic theory to predict extinction in these flames [11]. These studies have revealed that the scalar dissipation rate can be used as the fundamental parameter for evaluating extinction in diffusion flames.

The scalar dissipation rate provides a critically important mixing time scale for the analysis of diffusion flames. Damköhler number arguments are often used where this time scale is compared with the reaction time scale to determine if extinction events will occur. This scalar dissipation rate based approach for extinction analysis is favored in engine applications where small flow time scales are generated within and around the flame to enhance mixing. These small mixing time scales can fall below the time required to complete reaction resulting in flame extinction. In accidental fires, relatively long flow time scales with associated small scalar dissipation rates are assumed to exist and the effect of the flow on extinction are ignored. Instead, simpler thermal arguments are commonly used to predict extinction, such as defining a limiting critical flame temperature. In this study, scale analysis is used to establish scalar dissipation rates and associated flow time scales in accidental fires to evaluate the suitability of thermally based extinction arguments where flow effects are ignored. A more general critical scalar dissipation rate based approach for predicting extinction in accidental fires is also developed from evaluation of experimental data and numerical analysis of opposed flow diffusion flames.

2. KINEMATIC SCALES IN FIRES

There are two areas of the flame in which the scalar dissipation rate is potentially at its maximum. At the base of the flame, large-scale entrainment phenomena dominate the mixing, resulting in relatively large values of scalar dissipation rate. At the flame tip, buoyant acceleration causes high velocities and turbulent motion that can also produce relatively large values of scalar dissipation rate. Characteristic values for the scalar dissipation rate at the flame tip can be established by coupling traditional plume scaling laws, turbulent scale analysis, and scaling laws derived from asymptotic flame sheet theory. However, determining the scalar dissipation rate at the base of the flame is more challenging, as the selection of appropriate scales in this region is unclear. Direct Numerical Simulations of flow behavior at the flame base are currently being conducted to obtain estimates of the scalar dissipation rate in this region.

It is of interest to estimate scalar dissipation rates in actual fires for comparison with critical values to determine if extinction will occur. The scalar dissipation rate is defined as

$$\chi = 2D_{th}(\nabla Z)^2 . \tag{1}$$

As previously discussed, this quantity provides a characteristic (inverse) mixing time scale for non-premixed reactants in the reaction zone. Recently, this quantity has been measured in high strain diffusion flames [12]. However, the spatial and temporal requirements for measurement of χ are extremely demanding. Measurement of this quantity is even more challenging in configurations relevant to accidental fires because of their large scale and the harsh fire environment. Although the scalar dissipation rate has been estimated to be small in fires [13], measurements of χ are not yet available in the fire environment. In lieu of these measurements, it is useful to estimate this quantity through scaling arguments.

Scaling arguments are provided below to estimate the scalar dissipation rate in a pool fire. Reference values are provided in parenthesis corresponding to a 1 m diameter methane pool fire. The reference configuration represents a relatively large, but typical, accidental fire size (based on energy release rate) that may occur within a room. The large-scale fire behavior is described by the energy release rate,

$$\dot{Q} = \Delta h_c \frac{\pi D^2}{4} \dot{m}''_\infty (1 - e^{-kBD})(= 2.0\text{MW}) , \tag{2}$$

with the known fuel dependant parameters $\Delta h_c = 44,600\text{kJ/kg}$ is the heat of combustion of the fuel, $\dot{m}''_\infty = 0.101\text{kg/m}^2\text{s}$ is the mass flux for an infinite diameter pool, and $kB = 1.1\text{m}^{-1}$ is the product of the extinction absorption coefficient of the flame (k) and the mean beam length corrector (B) as described by Babrauskas [14]. The mean centerline velocity at the flame tip can be approximated by

$$u_{0,\text{max}} = 0.54(\Delta T_0 \frac{\dot{Q}}{1000})^{1/5}(= 9.1\text{m/s}) , \tag{3}$$

where $\Delta T_0 = 650\text{ K}$ is the increase in temperature at the flame tip [14]. The turbulent integral length scale is assumed to be directly proportional to the pool diameter so that

$$l_t = 0.5D(= 0.5\text{m}) . \tag{4}$$

The flame height is another possible length scale. In a pool fire, these length scales are closely related and of the same order. The pool diameter is chosen in this analysis for simplicity. In fires, the root mean square (RMS) velocity fluctuation is proportional to the mean centerline velocity $u' = 0.3u_{0,\text{max}} (= 2.8\text{m/s})$ as reported by Heskestad [15]. These integral quantities are useful for determining the Kolmogorov scales describing the smallest scales of turbulent motion. Because diffusion flames are known to be thin, these Kolmogorov quantities are appropriate for describing interactions with the flame. The Kolmogorov scales are given by

$$\text{Re}_t = \frac{u'l_t}{\nu}(=1720), \tag{5}$$

$$\eta_k = l_t\,\text{Re}_t^{-3/4}(=1.9\text{mm}), \tag{6}$$

$$\text{and } V_k = u'\,\text{Re}_t^{-1/4}(=0.42\text{m/s}) \tag{7}$$

where the viscosity is given by

$$\nu(T_{amb} + \Delta T_0) = \nu_{amb}\left(1 + \Delta T_0/T_{amb}\right)^{1.7}(=7.9\times10^{-4}\text{m}^2/\text{s}) \tag{8}$$

where ν_{amb} is the kinematic viscosity of air at standard temperature and pressure. This expression accounts for the significant change in viscosity due to the high bulk temperature at the flame tip. It has been established that the strain rate scales with the inverse of the Kolmogorov time scale yielding

$$a_t \sim 1/\tau_k = V_k/\eta_k(=225\text{s}^{-1}). \tag{9}$$

Furthermore, Yeung et al. determined that the mean strain rate can be approximated by

$$a_t = 0.28\tau_k(=63.0\text{s}^{-1}) \tag{10}$$

in their DNS analysis conducted over a range of *Re* [16]. The strain rate estimated for the 1m methane pool fire is small compared with strain rates generated in engines. The scaling argument produces strain rates that are consistent with the conventional understanding that strain rates are relatively small in fires.

The scalar dissipation rate can be determined from the strain rate and stoichiometric mixture fraction using an expression obtained from asymptotic analysis [10] combined with a correction factors, φ, to account for variations in mass density [17] yielding

$$\chi_{st} = \frac{a_t}{\pi}\varphi\exp[-2(\text{erfc}^{-1}(2Z_{st}))^2](=2.86\text{s}^{-1}), \tag{11}$$

where

$$\varphi = \frac{3((\rho_{O2}^\infty/\rho_{st})^{1/2}+1)^2}{4(2(\rho_{O2}^\infty/\rho_{st})^{1/2}+1)}(=1.56). \tag{12}$$

Ideal gas densities are used for air where, $\rho_{O2}^\infty/\rho_{st} = T_{st}/T_{O2}^\infty$, with $T_{O2}^\infty = 300$ K and $T_{st} = 2000$K assumed as characteristic temperatures. It is important to note that the oxidizer density could be evaluated at either ambient temperature or the bulk temperature at the flame tip. The ambient temperature was used to capture the extreme scalar dissipation events. This scaling argument provides an estimate for characteristic values of the local scalar dissipation rate at the flame tip. In this analysis the scalar dissipation rate at the flame tip is completely specified by the pool diameter and fuel properties. Figure 2 illustrates the effect of pool diameter on χ_{st} at the flame tip using methane as the fuel. It is apparent from Figure 2 that for large diameter pool fires, the characteristic scalar dissipation rate at the flame tip is well below the non-vitiated extinction scalar dissipation rate having a density corrected value of $\chi_{st}^{ref} = 11.2$ s^{-1} determined from OPPDIF analysis and Eq. (12). Even when increasing the pool diameter to 10 m, the strain rate does not exceed 100 s^{-1} and produces a correspondingly small scalar dissipation rate having a value less than 40% of that required for extinction. This scale analysis supports commonly accepted assumptions suggesting that buoyancy induced turbulence will result in relatively small scalar dissipation rates and that flame extinction in fires is unlikely, unless air vitation effects are accounted for. The importance of scalar dissipation rate effects on extinction criteria for fires will be evaluated in the following sections.

3. EXTINCTION CRITERIA FOR VITIATED FIRES

The two fundamental quantities used in extinction analysis are the scalar dissipation rate at the flame, χ_{st}, and the flame temperature, T_{st}. In the conventional view, the diffusion flame extinction condition is achieved by increasing the scalar dissipation rate through increases in reactant velocities until a limiting condition is reached as described in Figure 3. The governing quantities χ_{st} and T_{st} are modified together in this approach through changes in the strain rate, $a_g = (U_{O_2}^\infty / d)[1 + (U_f^\infty / U_{O_2}^\infty)(\rho_f^\infty / \rho_{O_2}^\infty)^{1/2}]$. However, an alternative pathway can be conceived to allow for independent variation of these two quantities. In this approach the temperature is reduced through changes in the reactant composition while maintaining a constant χ_{st} as shown in Figure 4(a) and as described by the Burke-Schumann flame temperature model:
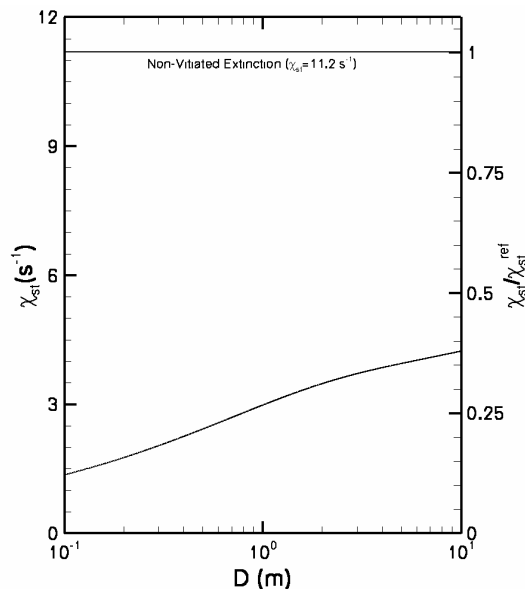

Figure 2: The mean scalar dissipation rate at the flame tip for methane as a function of pool diameter from the scaling analysis.
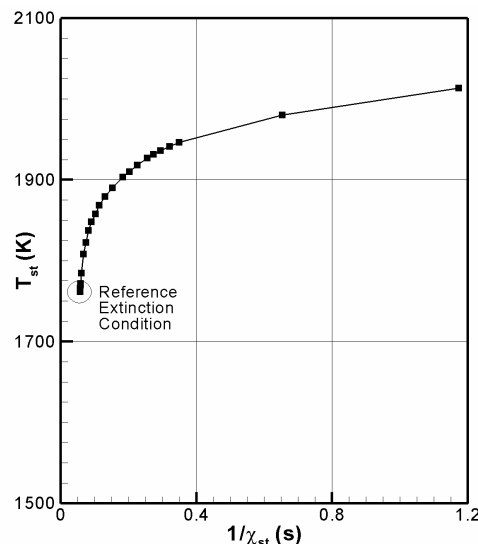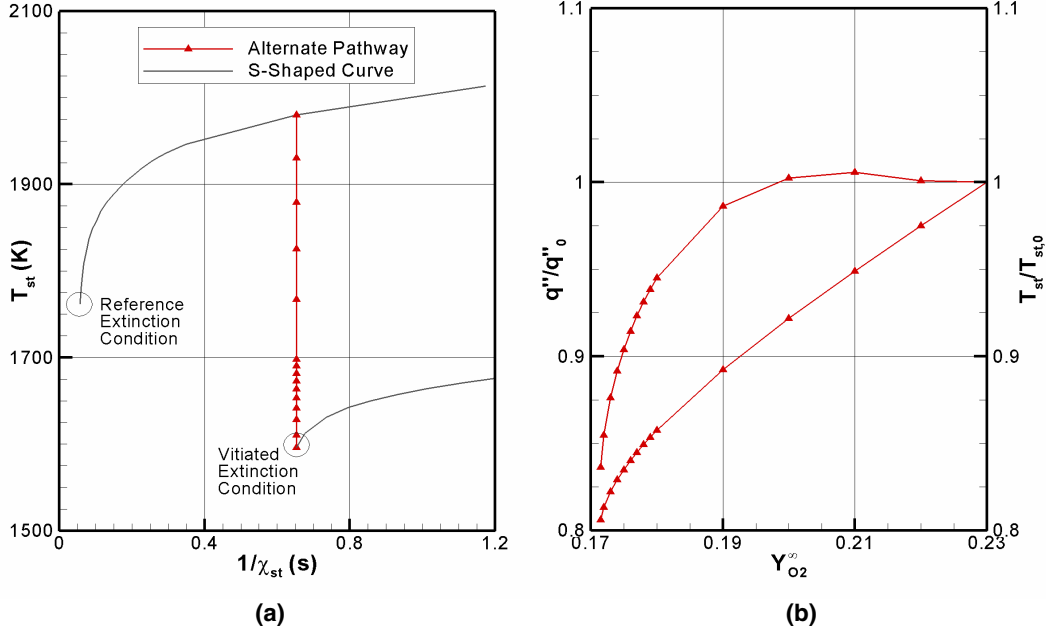

Figure 3: Reproduction of the upper branch of the classical S-shaped extinction curve with OPPDIF simulations. This pathway illustrates flame behavior by varying scalar dissipation rate with constant reactant properties $T_{O2}^\infty = T_f^\infty = 300 \text{ K}$, $Y_f^\infty = 1$, $Y_{O2}^\infty = 0.23$.

Figure 4: (a) Illustration of a vitiated constant scalar dissipation rate pathway to extinction. (b) Description of flame energy flux and stoichiometric temperature along the constant scalar dissipation rate pathway where $T_{O2}^\infty = T_f^\infty = 300\ \text{K}$, $Y_f^\infty = 1$, $\chi_{st} = 1.53\ \text{s}^{-1}$, $T_{st,0} = 1980\ \text{K}$, **and** $q_0'' = 2.06 \times 10^4\ \text{W/m}^2$ **from OPPDIF.**

$$T_{st} = T_f^\infty \frac{(Y_{O_2}^\infty / r_s)}{Y_f^\infty + (Y_{O_2}^\infty / r_s)} + T_{O_2}^\infty \frac{Y_f^\infty}{Y_f^\infty + (Y_{O_2}^\infty / r_s)} + \frac{\Delta h_c}{C_p} \frac{Y_f^\infty (Y_{O_2}^\infty / r_s)}{Y_f^\infty + (Y_{O_2}^\infty / r_s)} \tag{13}$$

where r_s is the stoichiometric air to fuel ratio and $\Delta h_c / C_p$ is the ratio of heat of combustion and constant pressure specific heat which is set to $3.55 \times 10^5\,\text{K}$ in order to produce the correct adiabatic flame temperature for methane burning in air. Figure 4 (b) shows that the flame intensity, q'' / q_0'' where q'' is the heat release rate per unit flame surface area, is nearly constant along this pathway as $Y_{O_2}^\infty$ and T_{st} are reduced until very close to the extinction condition where the q'' / q_0'' decreases abruptly. This on-off behavior along the constant χ_{st} extinction pathway is consistent with the relationship between the flame energy release rate and the scalar dissipation rate [19].

Because this study is focused on extinction in accidental fires and the reactants in accidental fires are often vitiated, it is critical to identify extinction criteria for various reactant compositions and temperatures. Following the laminar flamelet concept, the extinction of opposed flow diffusion flames is studied to characterize extinction behavior in accidental fires. The opposed flow flames are evaluated numerically using the OPPDIF code and experimentally using the opposed flow slot burner described in the Appendix. OPPDIF is an opposed flow diffusion flame code included in the detailed chemical kinetics software, Chemkinv4.1. OPPDIF solves the simplified partial differential equations describing opposed flow diffusion flames with detailed chemistry mechanisms provided by GRI mechanism 3.0 [19]. The OPPDIF simulations in this study do not include radiation effects.

In this study, numerical and experimental conditions are controlled to achieve extinction while maintaining a constant scalar dissipation rate. Extinction events are generated by fixing the oxidizer temperature while reducing $Y_{O_2}^\infty$ in the oxidizer stream (and correspondingly Z_{st}) and increasing the strain rate to maintain a constant value for χ_{st} (based on the expression from asymptotic theory provided in Eqs. (10-12)). Using this approach, extinction maps are generated in terms of oxidizer temperatures and oxygen concentrations at fixed scalar dissipation rates as shown in Figure 5.
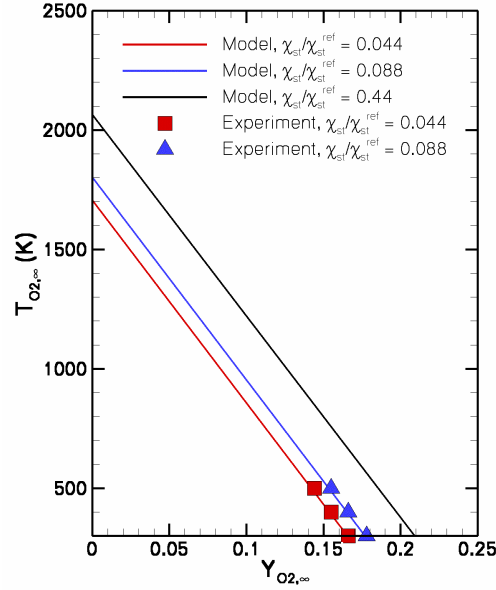
Figure 5: Extinction maps obtained experimentally and numerically from opposed flow flames generated at fixed scalar dissipation rates.

3.1. Scalar Dissipation Rate and Extinction

The Damköhler number, $Da = t_{mix}/t_{chem}$, is introduced to describe finite rate chemistry effects on flame extinction. Extinction occurs at subcritical Da where diffusive losses result in mixing times, t_{mix}, shorter than the characteristic reaction time, t_{chem}. The mixing time is inversely proportional to the scalar dissipation rate and the chemical time is inversely proportional to the Arrhenius rate. The critical Da concept thus provides an expression relating the critical scalar dissipation rate to the flame temperature given by

$$\chi_{st,crit} \sim \exp(-T_a/T_{st}) \tag{14}$$

where T_a is the activation temperature, and T_{st} is the stoichiometric flame temperature [10].

Addressing finite rate chemistry effects provides the basis to extend the description of extinction beyond the purely thermal formulation typically used in fire applications. In conventional fire analysis, the effects of oxidizer composition and temperature on the flame temperature (described in Eq. (13)) are considered; however the flame temperature is not used to determine a reaction time scale. Instead extinction events are determined by comparing this flame temperature with a specified critical value required to sustain the flame. Yet, scale analysis shows that the scalar dissipation rates in accidental fires can be significant resulting in relatively short mixing time scales. These short mixing time scales (possibly comparable to reaction time scales) suggest a need for a finite rate chemistry approach to account for the effect of flow conditions on extinction.

3.2. Critical Scalar Dissipation Rate Model

The critical scalar dissipation rate is related to the flame temperature as described by Eq. (13). In turn, this flame temperature is a strong function of the reactant composition and temperature. The critical scalar dissipation rate, $\chi_{st,crit}$, and associated critical reaction time scale is thus determined by the reactant composition and temperature.

It is important to realize that the mixture fraction variable used to analyze a typical compartment fire configuration is different from that used in a flamelet calculation as illustrated in Figure 1. At the system level, mixture fraction is a global variable that describes mixing between fuel and air, whereas at the flamelet level, mixture fraction is a local variable that describes fuel-air mixing near a particular flame element and under conditions that may be affected by air (or fuel) vitiation effects. In the following, we use Z to designate the global mixture fraction variable and Z^+ to designate its local

equivalent. Following the classical definition of mixture fraction, $Z = 0$ ($Z = 1$) corresponds to pure air (pure fuel) conditions. In contrast, in the flamelet analysis illustrated in Fig. 1, $Z^+ = 0$ ($Z^+ = 1$) corresponds to vitiated air (vitiated fuel). The relationship between the local and global definitions of mixture fraction is:

$$Z^+ = \frac{Z - Z_{O_2}}{Z_f - Z_{O_2}}$$

(15)

where Z_f (Z_{O_2}) denotes the value of (global) mixture fraction in the flamelet fuel (oxygen) supply stream. A consequence of this implicit renormalization of mixture fraction used in a flamelet analysis is that the values of the scalar dissipation rate need to be properly re-scaled for a correct interpretation back to the system level. We have the following relationship between the local and global definitions of scalar dissipation rate:

$$\chi_{st}^+ = \frac{\chi_{st}}{(Z_f - Z_{O_2})^2}$$

(16)

In the following, this expression will be used to map the local flamelet results back to global space.

Figure 6 shows OPPDIF and experimental extinction data taken at various oxidizer temperatures and oxygen concentrations. The OPPDIF extinction data in Figure 6(a) are plotted using the critical scalar dissipation rate, $\chi_{st,ext}$, and the flame temperature, $T_{st,ext}$ both defined at Z_{st}. It should be noted that OPPDIF derived scalar dissipation rates are modified based on Eq. (16) to determine $\chi_{st,ext}$. Recognizing that extinction occurs when chemical time scales are balanced with mixing time scales, the extinction data demonstrates strong Arrhenius correlation where the slope of the correlated data provides an activation temperature, T_a.
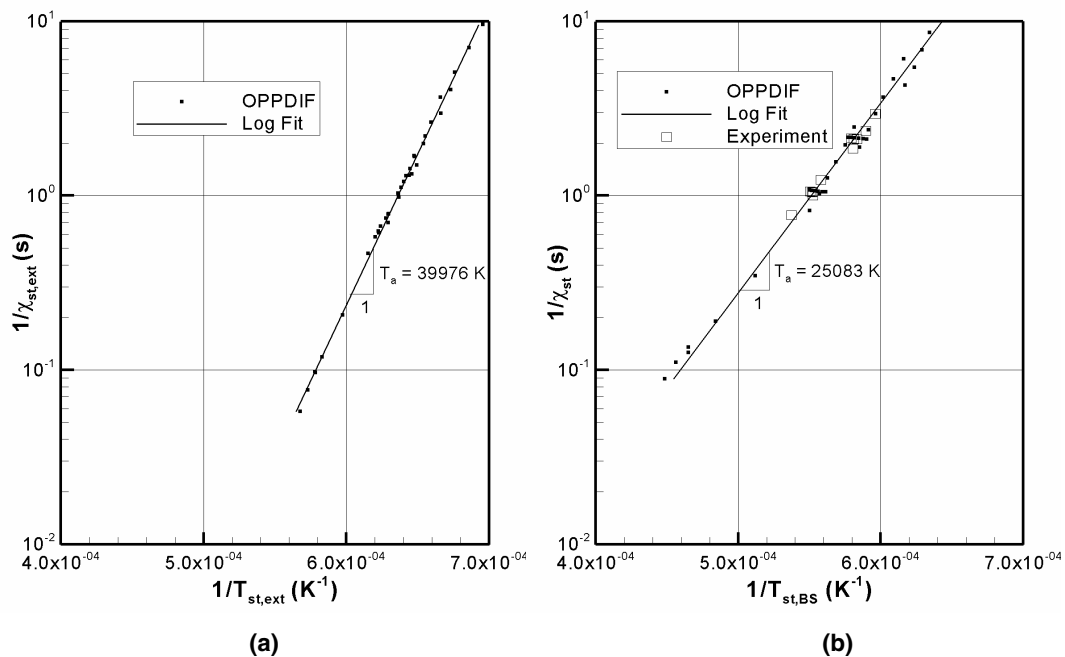
Figure 6: Describes various vitiated extinction conditions. (a) The $T_a = 39976 \, \text{K}$ data determined directly from OPPDIF. (b) The $T_a = 25084 \, \text{K}$ data describes OPPDIF and experimentally determined extinction conditions where T_{st} is determined from Eq. (13) and χ_{st} is determined from Eqs. (10-11).

Extinction events will occur when the local scalar dissipation rate at the flame

$$\chi_{st} \geq \chi_{st,crit}.$$

(17)

This critical scalar dissipation rate $\chi_{st,crit}$ can be established over a wide range of conditions using opposed flow experiments or opposed flow flame simulations with finite rate chemistry. The strong correlation between $\chi_{st,crit}$ and T_{st} demonstrated in Figure 6(a) suggests that it may be possible to determine $\chi_{st,crit}$ from more accessible quantities such as $T_{st,ext}$. The Burke-Schumann relationship described in Eq. (13) can be used to estimate the flame temperature in terms of the reactant composition. Furthermore, asymptotic diffusion flame theory provides a convenient alternative for estimation of the scalar dissipation rate based on the global strain rate and reaction composition as described in Eq. (10). These relationships provide convenient estimates of the extinction quantities in terms of easily determined inlet conditions offering the benefit of avoiding interrogation of the numerical solution or the experimental flame. The same extinction data is now used in Figure 6(b) where the scalar dissipation rate and flame temperature are described by $\chi_{st,crit}$ and $T_{st,BS}$, respectively. This formulation also shows strong Arrhenius behavior admittedly with more scatter than that exhibited from the plot obtained using the exact flame quantities $\chi_{st,ext}$ and $T_{st,ext}$. It should also be noted that the extinction data plotted based on inlet derived quantities provided a $T_a = 25083\,\mathrm{K}$, a value significantly different than that obtained from exact quantities.

Figure 7 clearly demonstrates the relationship between the flame temperature and the extinction scalar dissipation rate but a constant of proportionality is still required to determine the extinction scalar dissipation rate from the temperature. Following the approach proposed by Wang and Trouvé [16], the constant of proportionality can be avoided by normalizing Eq. (14) by a known value of the scalar dissipation rate at a reference extinction condition. The reference critical extinction value is the extinction point of the S-shaped curve from Figure 3(a) and is notated with superscript *ref*. A normalized extinction criterion in terms of the inlet derived extinction quantities is given by

$$\frac{\chi_{st,crit}}{\chi_{st,crit}^{ref}} = \exp\left[-T_a\left(\frac{1}{T_{st,BS}} - \frac{1}{T_{st,BS}^{ref}}\right)\right] \tag{18}$$

The extinction data is plotted once again in terms of inlet derived quantities in Figure 7(a). The reduction in $\chi_{st,crit}/\chi_{st,crit}^{ref}$ as the flame temperature is reduced indicates that the flame is becoming more vulnerable to extinction. The exponential expression on the RHS of Eq. (18) is also plotted as a solid line demonstrating that the critical scalar dissipation rate condition can be determined with reasonable accuracy from flame temperature estimates. As mentioned previously, Eq. (13) can be
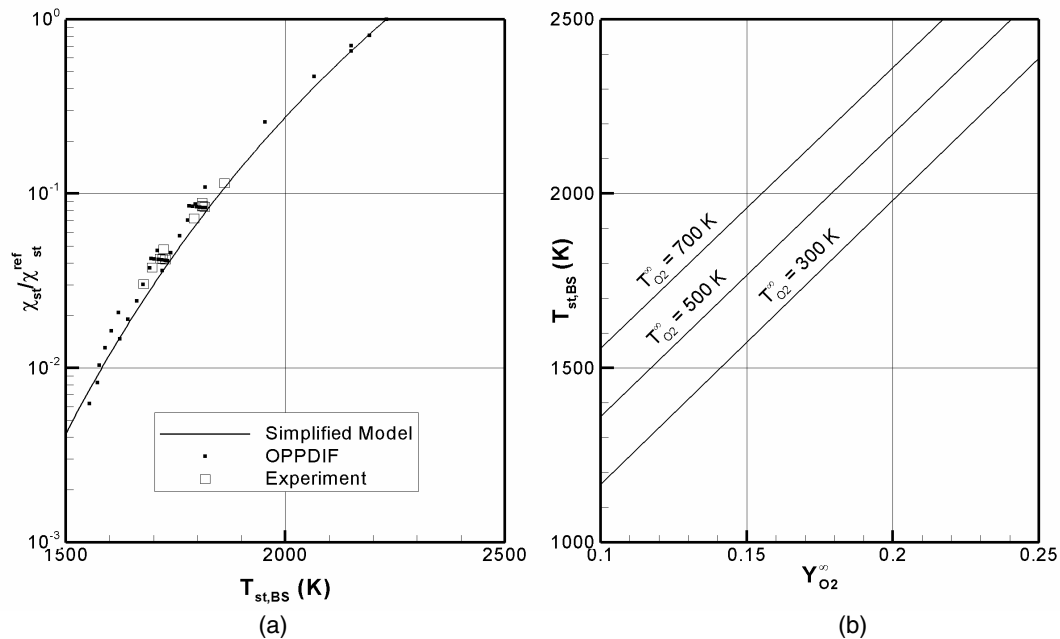

Figure 7: (a) Extinction data and model. (b) Burke-Schumann flame temperature model at various oxidizer temperatures, $T_f^\infty = 300\,\mathrm{K}$ and $Y_f^\infty = 1$.

used to estimate the flame temperature in terms of reactant composition and temperature. Figure 7(b) provides flame temperature estimates based on oxidizer temperatures and oxygen concentrations. Figure 7 thus provides an expanded view where vitiation effects in the oxidizer stream can be directly related to reduced flame temperatures and associated reductions in the critical scalar dissipation required for extinction.

4. CONCLUSIONS

Extinction criteria in fires have been critically evaluated in this study through scale analysis, numerical analysis of opposed flow flames, and experiments in an opposed flow slot burner. Scaling arguments suggest that extinction events are unlikely in open turbulent pool fires (w/o vitiation) even with large diameters. However, flames in actual fires exposed to vitiated conditions are more vulnerable to extinction. The impact of vitiation on extinction was the major focus of this study. Recognizing that both the mixing and chemical time scales are fundamental to the extinction problem, scalar dissipation rate based extinction criteria were established from numerical analysis and experiments. The oxidizer temperature, composition, and the scalar dissipation rate were independently varied to develop general extinction criteria valid over a wide range of conditions. Borrowing from ideas used in asymptotic diffusion flame analysis, the critical scalar dissipation rate required for extinction is provided in terms of the stoichiometric flame temperature, $T_{st,BS}$ and the associated oxidizer temperature and composition. This criterion was developed using a density corrected scalar dissipation rate, $\chi_{st,crit}$. A system level definition of the scalar dissipation rate where the mixture fraction is based on mixing between pure fuel and pure air was also used in the development of the extinction criteria. The extinction data show that the flame becomes increasingly vulnerable to extinction with reductions in $T_{st,BS}$ (i.e. reductions in T_{O_2} and/or Y_{O_2}). Furthermore, the results show that $\chi_{st,crit}$ can be determined from a known scalar dissipation rate at some reference condition, $\chi_{st,crit}^{ref}$, and the flame temperature, T_{st}, derived from the oxidizer temperature and composition. The critical scalar dissipation rate, $\chi_{st,crit}$, correlates with the extinction T_{st}, scaling with $\exp(-T_a/T_{st})$ consistent with the Da based perspective on extinction. From this relationship, it is evident that a critical extinction T_{st} specification strictly depends on the $\chi_{st,crit}$ determined from the local flame reactant composition and temperature (associated with the ventilation condition) *and* flame kinematics (associated with the size of the fire and fire dynamics).

NOMENCLATURE

a_g	Global Strain Rate (s^{-1})
a_t	Turbulent Strain Rate (s^{-1})
B	Mean Beam Length Corrector Factor
C_p	Constant Pressure Specific Heat (kJ/kg-K)
d	Separation Distance (m)
D	Pool Diameter (m)
Da	Damköhler Number
D_{th}	Thermal Diffusivity (m^2/s)

Subscripts

amb	Ambient Condition
BS	Burke-Schumann Model
$crit$	Extinction Condition (Modeled)
ext	Extinction Condition (Exact)
f	Fuel Property
O_2	Oxidizer Property
st	Evaluated at Stoichiometric Mixture Fraction

H_{st}^{*}	Enthalpy Deficit Parameter
k	Extinction Absorption Coefficient
l_t	Turbulent Integral Length Scale (m)
$\dot{m}_{\infty}''$	Reference Fuel Mass Flux (kg/m^2)
q	Local Energy Production (W/m^3)
q''	Flame Energy Flux (W/m^2)
$\dot{Q}$	Total Energy Release Rate (W)
r_s	Stoichiometric Air to Fuel Ratio
Re_t	Turbulent Reynolds Number
t_{chem}	Characteristic Chemical Time (s)
t_{mix}	Characteristic Mixing Time (s)
T	Temperature (K)
T_a	Activation Temperature (K)
$u_{0,\max}$	Mean Centerline Velocity at the Flame Tip (m/s)
u'	RMS Velocity Fluctuation (m/s)
U	Inlet Velocity (m/s)
V_k	Kolmogorov Velocity Scale (m/s)
x	Cartesian Coordinate (m)
Y	Mass Fraction
Z	Mixture Fraction

Superscripts

ref	Reference Condition
$+$	OPPDIF Parameter Space
∞	Vitiated Reactants

Symbols

β	Zel'dovich Number
χ	Scalar Dissipation Rate (s^{-1})
Δh_c	Heat of Combustion (kJ/kg)
ΔT_0	Temperature Increase at the Flame Tip (K)
∂	Partial Derivative
∇	Gradient
ϕ	Equivalence Ratio
φ	Variable Density Correction Factor
η_k	Kolmogorov Length Scale (m)
ν	Kinematic Viscosity (m^2/s)
ρ	Density (kg/m^3)

REFERENCES

[1] Quintere, J. G., *Proc. Comb. Inst.,* **29** (2002) 181-193.
[2] Takeda, H., and Kazuo, A., *Proc. Comb. Inst.,* **18** (1981) 519-527.
[3] Utiskul, Y., PhD Thesis, University of Maryland, (2006).
[4] Beyler, C. L., *Fire Safety J.,* **10** (1986) 47-56.
[5] Morehart, J. H., Zukoski, E. E., and Kubota, T., *Fire Safety J.*, **19** (1992) 177-188.
[6] Ishizuka, S., Tsuji, H., *Intl. Proc. Comb. Inst.,* **18** (1981) 695-703.
[7] Williams, F. A., *Turbulent Mixing in Non-Reactive and Reactive Flows* (1975) 189-208.
[8] Williams, F. A., *Fire Safety J.,* **3** (1981) 163-175.
[9] Sehadri, I. K., and Seshadr, K., **65** (1986) 137-150.
[10] Peters, N., *Comb. Sci. and Tech.,* **30** (1983) 1-17.
[11] Liñán, A., *Acta Astronautica,* **1** (1974) 1007.
[12] Donbar,, J. M., Driscoll, J. F., and Carter, C. D., *Comb. And Flame*, 125 (2001) 1239-1257.
[13] DiNenno, P. J., *The SFPE Handbook of Fire Protection Engineering*, (2002).
[14] Babrauskus, V., *The SFPE Handbook of Fire Protection Engineering*, (2002).
[15] Heskestad, G. *The SFPE Handbook of Fire Protection Engineering*, (2002).
[16] Yeung, P. K., Girimaji, S. S., and Pope, S. B., *Comb. And Flame*, 79 (1990) 340-365.
[17] William, F. A. *Prog. in Energy and Comb. Sci.* **26** (2000) 657 – 682.
[18] Peters, N. *Twenty-first Symp. (Intl.) on Comb.* (1986) pp. 1231-1250.
[19] Lutz, A., Kee, R., Grcar, J., Fupley, F., Sandia National Laboratories, SAND96-8243 (1996).

APPENDIX

A counter flow slot burner has been developed for this study as shown in Figure A.1. This burner was designed with the intended functionalities of achieving low flow rates, heated reactants and reactant concentration variability along the slot.
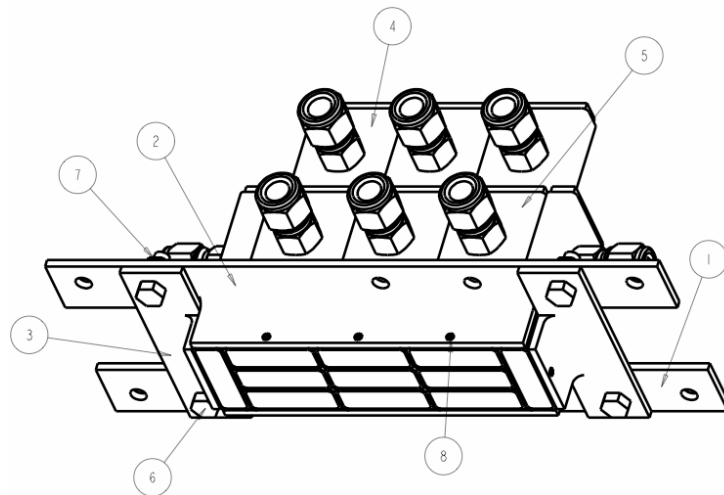
Figure A.1: Top injector of the UM Opposed Flow Slot burner. Oxidizer is injected along the central axis surrounded by N₂ co-flow.

The counter flow nozzle assembly is constructed almost entirely out of 316 Stainless Steel (SS) materials for high temperature resistance. Both the fuel and oxidizer nozzle assemblies consist of eleven individually fed nozzles, three of which are dedicated to reactant streams and the remaining eight are dedicated to nitrogen co-flow. Each of the individual nozzles is fabricated from 316 SS 1-½" by ½" OD and 0.062" thickness rectangular tubing. The tube is cut to length (5" for reactant nozzles and 3" for co-flow nozzles) and precision milled at the ends to produce a consistent end surface. One end is sealed and the other end of the tube is fitted with a bronze sintered (porous) metal insert 12 micron grade and 0.24" thickness. In order to minimize leak pathways, the inside of the tube is precision milled with 1/8" diameter end mill to ensure consistent and reproducible interior tube dimensions. The bronze sintered material is cut with an Electron Discharge Machine to +0.001" tolerance of the milled interior tube dimensions. The sintered metal insert is then friction fitted into the SS tube with a press. This method of fabrication produced the most consistent and reproducible plug flow velocity profile for each nozzle. The tube thickness on the ½" wall side is milled to reduced the separation distance of the nozzles to 0.05" total. The fuel and oxidizer nozzle assemblies are held in place by 1" by 1" by 1/8" thickness 90º angle bar, which allows for a compression force to the nozzles further reducing any possible variations from plug flow. The entire burner is mounted by an aluminum framing system that allows for alignment of both nozzle assemblies.

The mass flow rates of fuel and oxidizer are controlled by mass flow controllers with a maximum error of 1% of their full-scale reading. Inlet conditions are prescribed based on the Williams analytical expression for scalar dissipation rate that accounts for different inlet densities. The OPPDIF inlet conditions were prescribed using the same method. High temperature flexible heaters capable of operating up to 1000 K control the oxidizer temperature. The heaters are wrapped around the oxidizer nozzle assembly and heated to a steady state temperature as monitored by surface mounted thermocouples. During high temperature operation, the exit gas temperature was measured to be within 10 K of the measured surface temperature of the nozzles. Based on the temperature limitations of the bronze sintered metal material, heating of the burner is limited to 600 K to avoid oxidization of the insert. It will be possible to achieve higher burner temperatures if the bronze insert is replaced with a nickel alloy insert.

Flame extinction data is obtained from visual observations of the flame. The burner is operated at conditions along the constant scalar dissipation rate pathway at constant reactant temperatures. The oxidizer concentration is systematically decreased until the flame is extinguished. The extinction condition is defined as the lowest oxidizer concentration that allows for a stable flame at the prescribed reactant temperatures and scalar dissipation rate. The experiment is repeated at various oxidizer temperature variations and scalar dissipation rates.